Lembar Pengesahan Publikasi

1. Judul Jurnal : Civil and Environmental Research Journal
2. Nama Penulis : Chatarina Niken
3. Publikasi
    a. Nama Publikasi : The Evolution of Concrete (Part 1): Submerged in Water and Its Compression Strength
    b. ISBN/ISSN : 2225-0514
    c. Vol/ No/ Tgl/ Bln/Hal : 14/4/ 30/Juni/1-9
    d. Tautan : https://iiste.org/Journals/index.php/CER/article/view/58923/60838
       http://repository.lppm.unila.ac.id/id/eprint/43189
4. Penerbit : IISTE

Bandar Lampung, 21 Juli 2022

Mengetahui
Ketua Jurusan Teknik Sipil Unila

Ir. Laksmi Irianti, M.T
NIP: 196204081989032001

Penulis,

Dr. Ir. Chatarina Niken, M.T.
NIP 195806131984032003

Menyetujui
Ketua LPPM Unila.

Prof. Dr. Ir. Lusmeilia Afriani, D.E.A.
NIP 196505101993032008

Mengetahui,
Dekan Fakultas Teknik UNILA

Dr. Eng. Helmy Fitriawan, S.T., M.Sc.
NIP 197509282001121002

DAFTAR ISI

DAFTAR GAMBAR

DAFTAR TABEL

The Evolution of Concrete (Part 1): Submerged in Water and Its Compression Strength

Chatarina Niken *

Civil Engineering Department, Faculty of Engineering, Lampung University, Jl. Sumantri Brojonegoro No 1
Bandar Lampung, Indonesia
*E-mail of the corresponding author: chatarinaniken@yahoo.com

Abstract

This paper discusses about the water-submerged concrete on the concrete basemen that has been in the gorunding for about ten years. The purpose of this study was to determine the compressive strength and microstructural changes in water submerged concrete. The research was carried out experimentally. It was a case study at the State University Hospital, Lampung University, Indonesia. The compressive strength and microstructure of the submerged concrete compared to the concrete in the protected condition. The sample for the compression test was taken with a core drill 4 samples in each condition. The test data was processed by the outlying method. The microstructure of the concrete was examined by scanning electron microscopy (SEM), and energy-dispersive X-ray (EDX). The results showed that the compressive strength of submerged concrete was similar to the compressive strength of protected concrete. The elements that dominate the submerged concrete are Si and O, and in the protected concrete are Ca and O. The conclusion and novelty of this research are that submerged concrete can evolve into ceramics with SiO_2 as the main element and heterogeneous microstructure with the same compressive strength as protected concrete. This can be used as a reference and applied to concrete buildings that are in close contact with water such as dams, ponds, and other underwater structures. This research contributes to the science of concrete and its use, especially for underwater structures.

Keywords: compressive strength, concrete, evolution, microstructure, submerged in water.

1. Introduction

The compressive strength of concrete is the main property that is relied on in all concrete structures, including submerged concrete. Several researchers have paid attention to the mechanical properties of concrete. The compressive strength of concrete under marine environments with various saturation and salinity conditions has been studied [Candelaria *et al*. 2022]. The concrete stress in the saturated zone of the foundation is mainly caused by the alkali-silica reaction [Beyene & Meininger 2021]. The compressive strength of water-saturated concrete is lower than that of air-dried concrete [Ge *et al*. 2021]. The volumetric stiffness of saturated concrete is much higher than that of dry concrete [Huang et al. 2020]. The internal pore structure of the concrete pavement which is affected by high and low temperatures for a long-time changes, and causes a decrease in the mechanical properties of the concrete [Shi *et al*. 2020]. Compared with dry cement mortar specimens, the tensile strength of saturated cement mortar specimens is decreased by 23.36% [Gu *et al*. 2019].

Some concrete structures are intended as retainers and contain water so that during their service life they are submerged in water or contact with water. These buildings include dams, ponds, foundations in rivers, and piles in the sea.

Concrete is a porous material, so that the opened pores can be an entry point for water with or without pressure. It makes water or other particles can enter through it. The ability of water penetration into the concrete determines the level of permeability of the concrete. This is influenced by the pore radius and particle size [Hand *et al*. 2019]. The penetration of water under cyclic pressure into submerged concrete cylindrical specimens under different confinement conditions has been investigated [Fujiyama *et al*. 2019].

Incoming water can be bound to hydration products. Meanwhile, there is also free-moving water. The mobility of free water in the hardened cement paste microstructure has been at the center of a longstanding debate, motivated by the need to understand the underlying mechanisms that play a role in drying, deformation by shrinkage, creep, and thermal expansion [Wyrzykowski *et al*. 2019]. The concrete manifests different wet expansion deformations under the application of different temperatures if the hydraulic concrete is immersed in water [Huang *et al*. 2018]. Saturated concrete shows higher failure stress and a more important pores closing [Bian *et al*. 2017].

Certain phenomena that occur in submerged concrete cannot be detected through monitoring or visual inspection; numerical analysis is needed to confirm the existence of the phenomenon [Mohd *et al*. 2016].

Water enters the concrete, allowing some elements to enter, leave, and some bonds to break. For saturated concrete, a curing process has been carried out using the electrochemical deposition method by micromechanics taking into account the imperfections of the interface. An improved micromechanical framework at the interface

transition zone (ITZ) has been proposed as an improvement. A multiphase micromechanical model with ITZ was proposed based on the material microstructure and a new stratified homogenization scheme with interactions between particles to predict the effective properties of the improved concrete taking into account the effect of ITZ [Chen et al. 2016]. However, the compressive strength of saturated concrete, especially those with low water-cement ratio increases with increasing strain rate [Kaji & Fujiyama 2014]. Likewise, concrete that is immersed underwater tends to be stronger than concrete that sticks in the air [Wikipedia]. This statement contradicts to Ge et al, 2021 [Ge et al. 2021].

In saturated concrete pores, the oxygen available at the noncorroding site is limited because oxygen must diffuse through the concrete pore water. Corrosion reactions occur at optimal water content. In the splash zone, concrete breaks down very rapidly where moisture and oxygen are abundant in non-rusting locations [Shi et al. 2020].

Based on the description above, it is necessary to study the microstructure and compressive strength of submerged concrete.

2. Material and Method
2.1 Materials
This research was conducted with a case study on the Basement Floor of the State University Hospital (RSPTN) of the University of Lampung in Lampung Province, Indonesia. This building has been abandoned for 10 years. Part of the basement floor is protected and partly submerged in water (Figure 1).
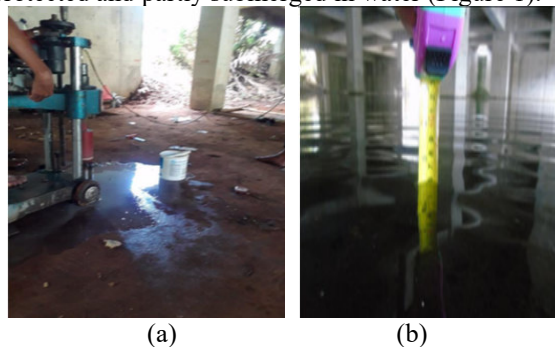

(a)   (b)

Figure 1. Basement conditions: (a) protected, (b) submerged in water

There are 4 samples which are taken by core drill method for each condition. This sample was used for compressive strength testing (Figure 2).

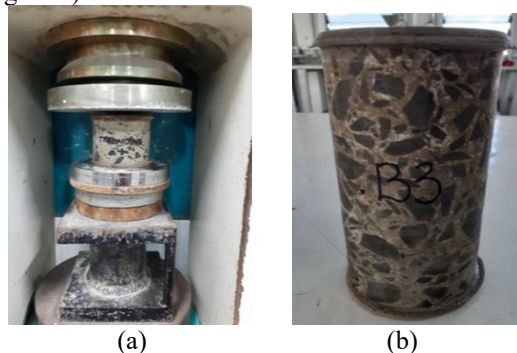(a)   (b)

Figure 2. Drill core samples: (a) protected, (b) submerged in water

Concrete chips in each condition were also taken for scanning electron microscopy (SEM) and energy-dispersive x-ray spectroscopy (EDX) tests.

2.2. Method
Four compressive strength data from each condition were processed using the Dixon criteria method [ASTM E178, 2002]. The samples were taken for testing SEM, EDX (relationship between atom energy and dynamic viscosity), and atomic mass. SEM data were observed at magnitudes of 2.00 K, 5.00 K, 10.00 K, and 15.00 K. The purpose of using various magnitudes is so that all forms of microstructure are not missed.

EDX and SEM results were analyzed and integrated. The results are related to the compressive strength results.

3. Result
3.1 Compression strength
Data acceptance is carried out by examining the largest and smallest values by comparing the values at the 5%

significance level. The results of this comparison can be seen in Figure 3. Because the results of processing the largest and smallest values are less than the 5% significance level, all data are accepted. Thus; the compressive strength can be calculated from the average data (Figure 4).
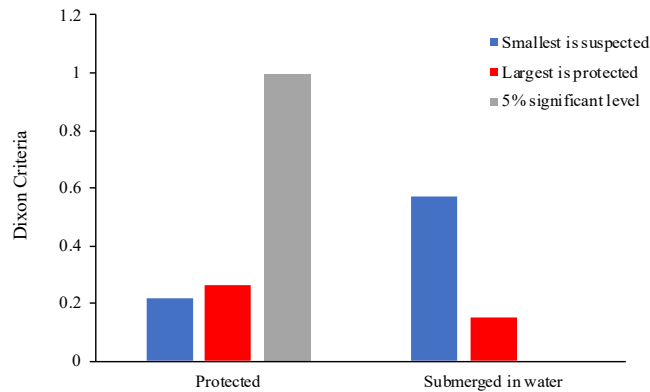

Figure 3. Checking the data using the outlying method
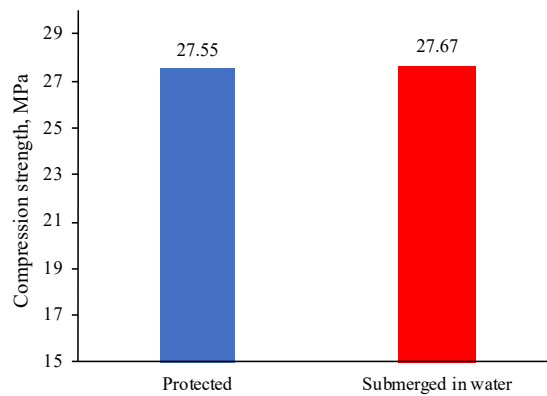
Figure 4. Concrete compressive strength of Protected concrete, and concrete submerged in water

3.2 Energy dispersive X-ray spectroscopy
The relationship between energy, dynamic viscosity, and atomic mass of the EDX results can be seen in Figure 5.
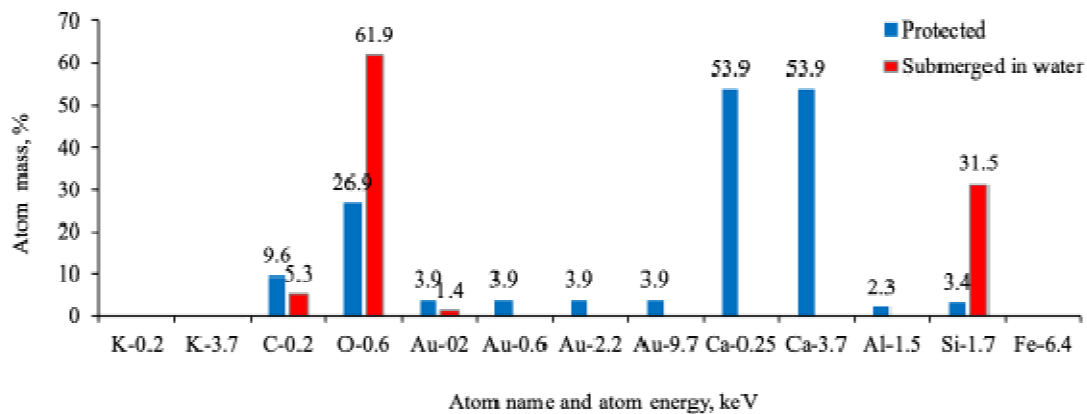
Figure 5. Atom mass of protected and submerged in water concrete

The results of scanning electron microscopy with magnitudes of 2.00 K, 5.00 K, 10.00 K, and 15.00 K under-protected and submerged conditions are presented in Figures 6.1 to 6.4.
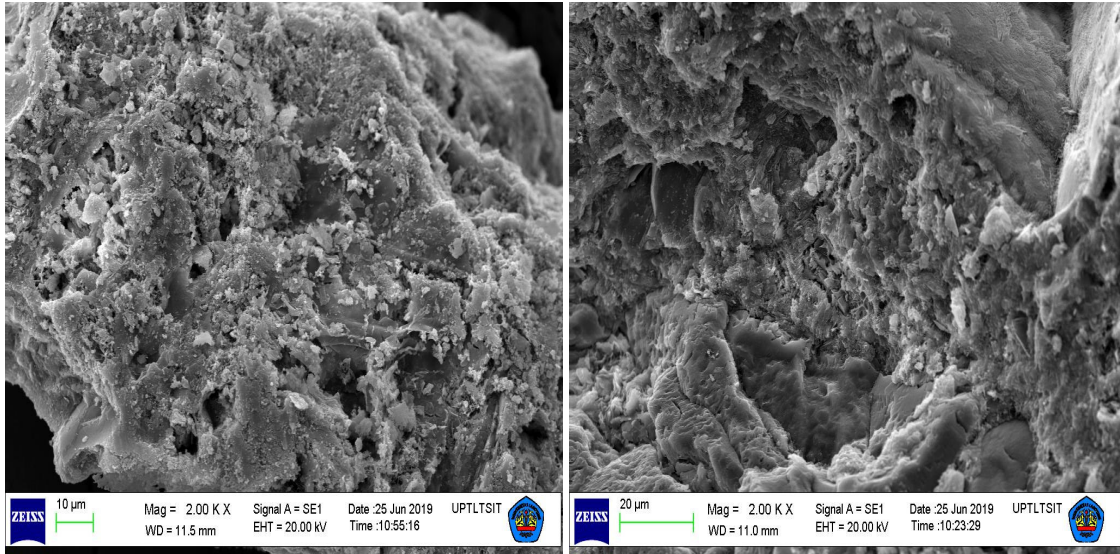
(a)   (b)

Figure 6.1: (a). Protected, (b). Submerge in water with Mag of 2.00 K
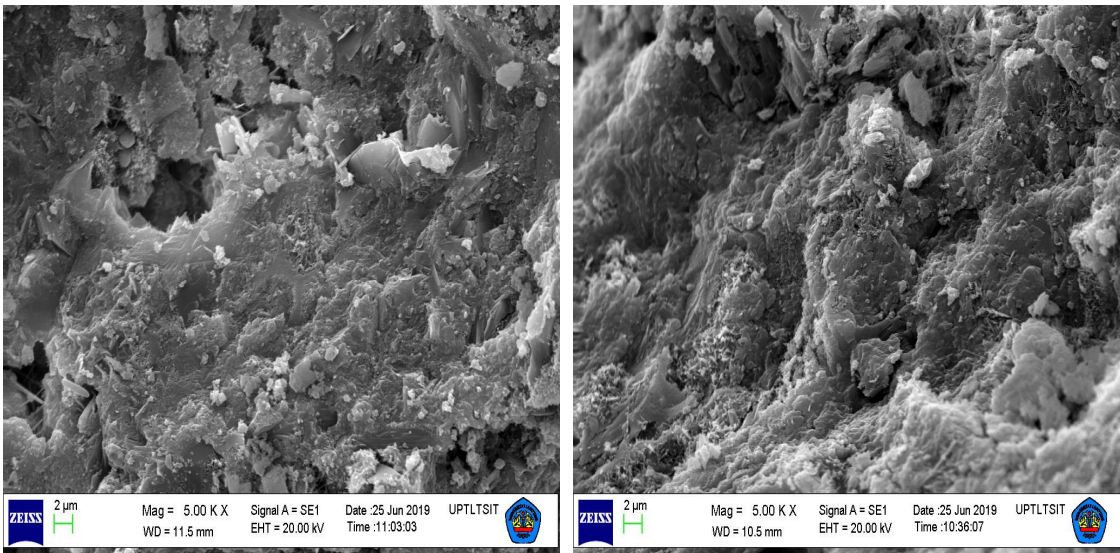
(a)   (b)

Figure 6.2: (a). Protected, (b). Submerge in water with Mag of 5.00 K

(a)   (b)

Figure 6.3: (a). Protected, (b). Submerge in water with Mag of 10.00 K

(a)   (b)
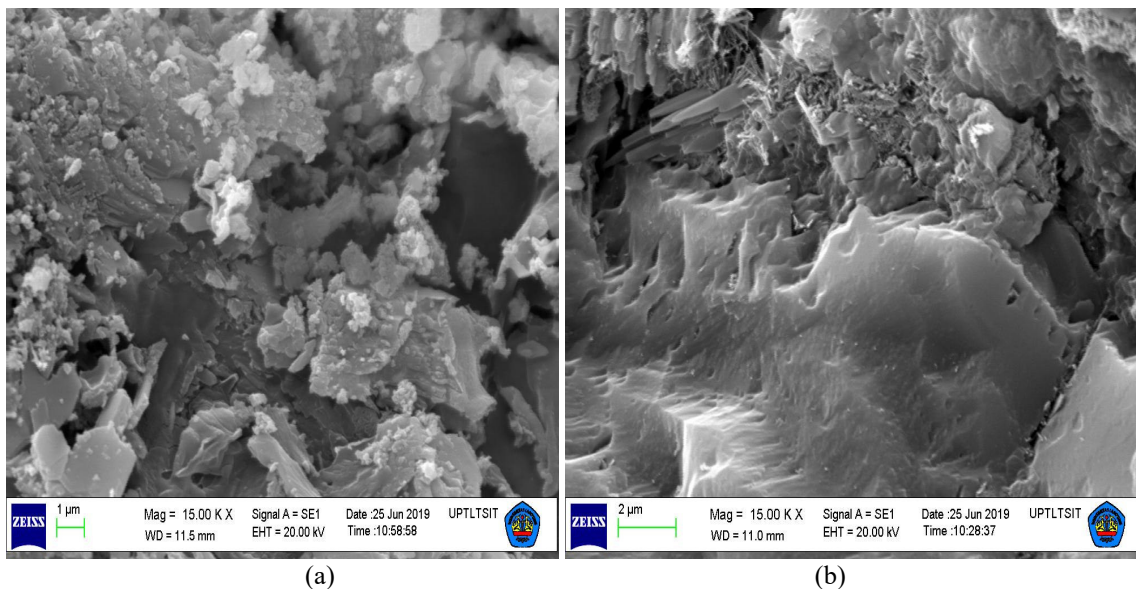
Figure 6.4: (a). Protected, (b). Submerge in water with Mag of 10.00 K

The differences in the protected and submerged microstructure at various magnitudes are presented in Table 1.

Table 1. Differences in microstructure of protected and submerged concrete

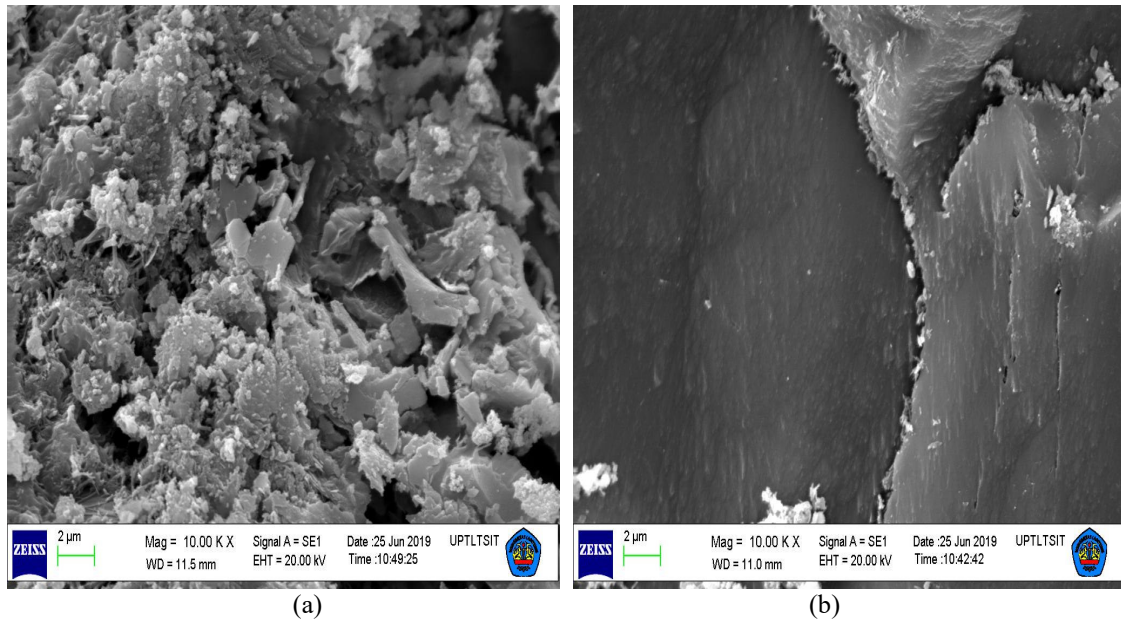| Magnitude	Surface View	
	Protected	**Submerged in water**
2.00 K	Coarse & massive, small pores	Some are rough, some are smooth, some are massive, some have large pores
5.00 K	CH crystal, CSH, deep visible pores	Some are smooth, some are rough, the pores are shallower
10.00K	CH and CSH look very massive, with many pores and deep	Fine areas overlap each other, deep pores. This picture shows only the smooth part, the rough part is not visible
15.00K	CH and CSH are very massive, deep pores	Sharp edges on smooth and even parts, flat parts that overlap each other, fine lumps, coarse, shallow pores, more homogeneous

4. Discussion

Cement-based materials have a complex multi-component structure that is formed immediately through a

chemical reaction. It continues to change over time and under environmental conditions. Protected concrete conditions are concrete conditions that are not exposed to the sun-light and rain directly. The uncontaminated concrete has the main hydration products of calcium silicate hydrate (CSH), and portlandite (CH).

From the SEM results of protected concrete, it can be seen the presence of the main hydration product. Small and deep pores are also clearly visible (Figures. 6.1a, 6.2a, 6.3a, 6.4a). The atomic mass of Ca in the protected concrete is quite high but the atomic mass of Si is low (Figure 5).

In submerged concrete, the water that soaks the concrete is surface water and rainwater. Rainwater contains water vapor, nitric acid, carbon, salt, and sulfuric acid.

4.1 The process of micro-evolution of protected normal concrete structures into submerged concrete

Concrete is a porous material. These pores are formed because air is trapped during mixing or in the air-entrainment process, which aims to spread pores with a diameter of 50 nm to make them more resistant to freezing. The number of pores is spread at the beginning of mixing. It decreases until it reaches a certain value as it matures.

The pores are the entrance to water. The water and particles that enter it make the concrete evolve. Pores greater than 10nm are often present in concrete. There are two classes of pore properties, between 10-20 nm starting when the material reaches a solid hyperstatic state and second around 1-2 nm. The first relates to the pore space of the CSH hydrate cluster and the second relates to the internal porosity of the hydrate [Morin *et al*. 2002]. Nanometer-scale internal pores are presented in CSH. The distribution of pores in the concrete can be seen in Figure 7.
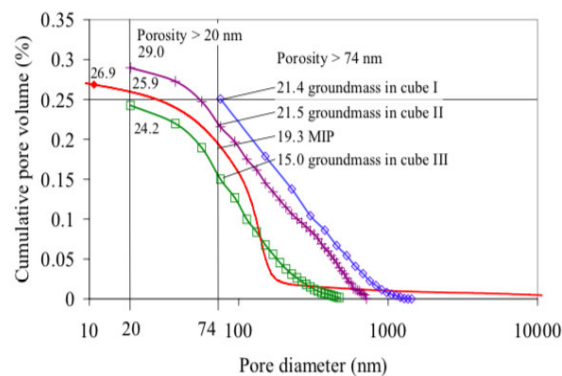
Holzer et al. 2006
Figure 7. Distribution of pores in concrete

The pore size of the concrete is spread from 10 nm to 1000 nm (Figure 7), while the size of the H_2O atom is 2.75 Angstrom, so water can easily enter the concrete even in the interlayer space (< 0.5nm), thus the pores in the submerged concrete are 100% saturated.

Water enters through open pores, and continues to move in the concrete pores, making CH dissolved and then removed [Lagerblad, 2001]. The submerged condition makes Ca cannot be bounded to the surface but it continues to be removed and depleted. As a result of the depleted Ca, CSH and CH also disappear, what is left is Si, O, C and Au. The energies of atom C, O, Au and Si are the same between protected concrete and submerged concrete (Figure 5).

4.2 Microstructure type

There are three types of submerged concrete microstructure (Figure 6.4.b). The first type dominates this microstructure, which is wide and flat with a pointed tip, the second type is in the form of a cloud-like lump with a smooth but uneven surface. The third type is a long groove containing a rough section and needle structure (Figure 6.4.b). This microstructure is in line with condition as shown in Figure 8 [Lagerblad, 2001].

4.3 Pressure by stagnant water

Water soaks the concrete from one side. Because water enters from one side, the evolution of concrete is not the same between the layer near the top surface of the concrete and the part far from the top surface of the concrete. There was the dissolution of clinker grains and CH in the layer close to the top surface of the concrete, and in the part far from the top surface of the concrete densification occurred (Figure 8).
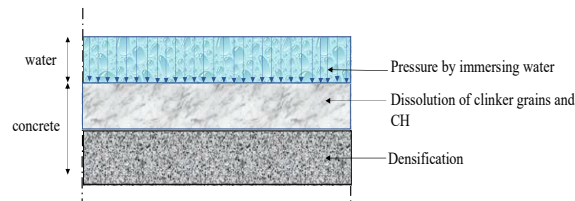
Lagerblad, 2001

Figure 8. Concrete layer submerged in water on one side

The one-way pressure of stagnant water added by rainwater makes the pore network more congested. The scheme of the pore network with the compressive force of water can be seen in Figure 9.
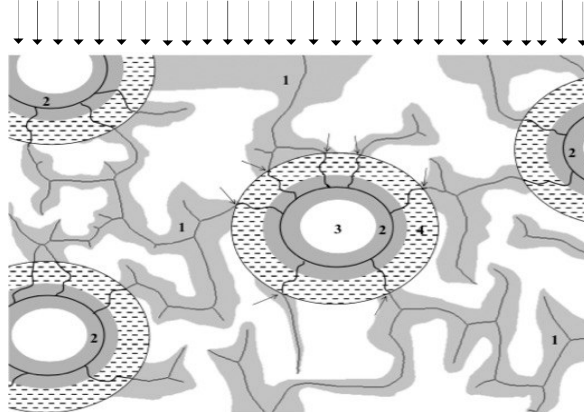
Holzer et al, 2006

Figure 9. Schematic illustration of a pore network, (1) Capillary pores, (2) Phaenograins with porous zones, (3) Un-hydrated clinker, (4) Dense hydration layer

The pressure from the stagnant water hits the pore network. The pressure keeps the water in the pores of the concrete moving. This pressing movement causes some of the pores to rupture, nor the pore water disperses, and some of the other pore water displaces the pore walls. By this pressure, pore water can reach un-hydrated clinker in the dissolution zone of clinker grains and CH and the densification zone and hydration process occur. The maximum chemical activity is the transition between pore classes 1 and 2 [Morin *et al.* 2001]. The evolution of the active capillary radius occurs. The phenomenon as a function of the degree of hydration indicates a strong interaction between capillary network size and chemical activity [Morin *et al.* 2001]. This reaction occurs under pressure. Chemical reactions that occur under pressure make the concrete expand abnormally [Van Vlack, 1973]. The surface of Si and O becomes shaped like a smooth lump which by the pressure and friction that occurs becomes increasingly smooth, wide, flat, and overlaps with one another. The hydration products of ettringite appear needle-like in the groove region (Figure 6.4b).

The exterior of the hydrated cement (Figure 9) contains pores. The presence of pore water keeps the clinker hydrated. Both the already formed and newly formed pores are immediately pressured by the inundated water and becomes clogged.

Friction sometimes stops when there is no additional pressure such as rain and makes the edges of the smooth and flat part have a distinctive or pointed shape. The compressive and frictional forces make the originally deep pores shallower. The atomic masses of C and Au show small values, appearing as small, rough spots (Figure 6.4b). However, because the water is always inundated, the Ca resulting from the hydration reaction dissolves and is lost, while Si adds to the solids. The reaction also grows pores.

4.4 Oxygen

Some of the water that inundates the concrete is surface water so there is more oxygen. Si and Al move freely due to oxidation and change their atomic coordination [Lagerblad, 2001]. The pressure will reduce the mobility of Si and compress the pore that formed. So that, this mechanism makes the pore shallower.

The above mechanism makes the atomic masses of Si and O under water submerged to 2.3 and 9.4 times the protected condition, respectively (Figure 5). This shows that the Si and O concrete submerged in water experienced significant densification.

4.5 Carbonat

The surface water also contains carbonates, bicarbonates, carbon dioxide and sometimes sulfates and Mg. Carbonate is also contained in rainwater. Carbonate and Mg that enter through water infiltration into the concrete form a physically stable surface, by means of which Mg replaces Ca [Lagerblad 2001]. This makes Mg non-

existent and the Ca formed then undergoes leaching until it is exhausted because the concrete is submerged in water (Figure 5). When Ca drops, the pH of the concrete can exceed 10.5: under these conditions the sulfate reacts with the aluminates and forms ettringite (Figure 6.4.b).

The water that soaks the concrete makes the carbonate eroded and lost to the water so that the atomic mass of C in the submerged condition is smaller than the atomic mass of C in the protected condition (Figure 5).

Diffusion of carbonate ions into the paste giving a carbonate surface enrichment in the silicate gel and some of it is lost to water.

4.6 Compression strength

The compressive strength of protected and submerged concrete can be said to be the same because it is only 0.12 MPa difference (Figure 4). The compressive strength of the concrete is protected mainly from the contribution of CSH and CH. The protected condition concrete showed higher Ca and O atomic masses than the submerged concrete (Figure 5). Ca atoms in unprotected concrete do not experience leaching, so Si becomes stable. The consequence of this condition CSH is also stable. The stability of CSH and CH can be seen from the microstructure in the protected condition (Figure 6.1a, 6.2a, 6.3a, 6.4a) which is denser with deeper pores than the submerged condition (Figure 6.1.b).

The elements Si and O dominate the submerged concrete. SiO_2 is also a ceramic element. Compressive strength of pure SiO_2 is 1100-1600 MPa [AZO, 2011]. SiO_2 can also be used as an additive in ceramics. With the main element aluminum sample with 10% SiO_2 additive and a sintering temperature of 1400°C, shows a maximum density value of 2.59 g/cm³, a minimum porosity of 10% and the highest compressive strength of 234.60 MPa [Nasrun & Sujianto, 2020]. Thus; Si and O make a major contribution to the compressive strength of submerged concrete. The compressive strength of the submerged concrete is 27.67 MPa (Figure 4). This value is far below the value of Nasrun and Sujianto, 2020. The low compressive strength is due to the influence of aggregate, interfacial transition zone, and heterogeneous microstructure although SiO_2 dominates.

5. Conclusion

The microstructure of the submerged concrete has been studied. The microstructure of the submerged concrete describes the non-uniform condition of the concrete. This is in accordance with [Lagerblad, 2001]. Water-submerged concrete can evolve into ceramics with the main element SiO_2.

The compressive strength of water-submerged concrete is the same as that of protected concrete one.

References

ASTM E178-02 (2002), "Standard Practice for Dealing with Outlying Observation", ASTM International, West Conshohocken, Pennsylvania: ASTM International.

AZO Materials (2011), "Engineering Ceramic Microstructures and Machining".

Available from: https://www.azom.com/article.aspx?ArticleID=5697

Beyene, M., & Meininger, R. (2021), "A Case Study of Distress Mechanism(s) in a Concrete Structure Foundation in the Saturated Zone and Above the Saturated Zone", *Journal of Microscopy. 284(1)*.

Bian, H., Jia, Y., Pontoroli, C., & Shao, J-F. (2017), "Numerical Modeling of the Elastoplastic Damage

Behavior of Dry and Saturated Concrete Targets Subjected to Rigid Projectile Penetration", *Numerical and Analytical Methods in Geomechanics Journal*, 42 (2), 312-338.

Candelaria, M.D.E., Kee, S.-H., & Lee, K.-S. (2022), "Prediction of Compressive Strength of Partially Saturated Concrete Using Machine Learning Methods", *Materials Journal 15 (5)*, 1-25.

Chen, Q., Jiang, Z., Zhu, H., Ju, J.W., & Yan, Z. (2016), "Micromechanical Framework for Saturated Concrete Repaired by the Electrochemical Deposition Method with Interfacial Transition Zone Effects", *International Journal of Damage Mechanic*, **26** (2), 210-228.

Fujiyama, C., Koda, Y., & Sento, N. (2019), "Degradation of Submerged/wet Concrete under Cyclic Compression and Cyclic Shear". *MATEC Web of Conferences*, 258, 05012, 1-7.

Ge, P., Huang, W., Zhang, H., Quan, W., & Guo, Y. (2021), "Study on Calculation Model for Compressive Strength of Water Saturated Recycled Aggregate Concrete", *KSCE Journal of Civil Engineering*, **26**, 273-285.

Gu, C., Xu, J.Y., & Meng, B.X. (2019), "Effect of Saturation on Mechanical Behavior of Cement Mortar Based on 8-Type Tensile Test", 3rd International Workshop on Renewable Energy and Development", *IOP Conference Series: Earth and Environmental Sciences*, 267, 022003, 1-7.

Hand, D., Wang, Z., Wang, Q., Wu, B., Yu, T., & Wang, D. (2019), "Analysis of the Kozeny-Carman Model

Based on Pore Network" *Journal of Geophysics and Engineering*, *16 (6)*, 1191-1199.

Holzer, L., Gasser, P., & Muench, B. (2006), "Quantification of Capillary Pores and Hadley Grains in Cement Paste Using FIB-Nanotomography: Measuring, Monitoring and Modeling Concrete Properties". *2nd International Symposium on Advance in Concrete through Science and Engineering*, 509-516.

Huang, X., Kong, X., Chen, Z., Fang, Q., & Peng, Y. (2020), "Equation of State for Saturated Concrete: A Mesoscopic Study", *International Journal of Impact Engineering*, *144*. 103669

Huang, Y., Yuan, B., Xiao, L., & Liu, Y. (2018), "Studies on the Wet Expansion Deformation of Hydraulic Concrete with Fly ash under Non-standard Temperatures", *Case Studies in Construction Materials Journal*, *8*, 392-400.

Kaji, T., & Fujiyama, C. (2014), "Mechanical Properties of Saturated Concrete Depending on the Strain Rate", *Procedia Engineering Journal*, **95**, 442-453.

Lagerblad, B. (2001), "Leaching Performance of Concrete Based on Studies of Samples from Old Concrete Construction", Svensk Kärnbränslehantering AB Swedish Nuclear Fuel and Waste Management Stockholm Sweden, Technical Report TR-01-27, 1-83.

Mohd, M., Zainon, O., Rasib, A. W., & Majid, Z. (2016), "The Study on the Durability of Submerged Structure Displacement due to Concrete Failure". *The International Archives of the Photogrammetry, Remote Sensing and Spatial Information Sciences*, Volume XLII-4/W1, 345-350.

Morin, V., Cohen-Tenoudji, F., Feylessoufi, A., & Ricahard, P. (2002), "Evolution of the Capillary Network in a Reactive Powder Concrete During Hydration Process", *Cement and Concrete Research Journal*, **32**, 1907-1914.

Nasrun, M., & Sujianto, (2020), "Pembuatan dan Pengujian Sifat Fisis dan Mekanik Keramik Alumina sebagai Komponen Mekanik", Teknika: *Jurnal Sains dan Teknologi*, **16** (2)*, 249-254*.

Shi, J., Zhao, Y., & Zeng, B. (2020), "Relationship between Pore Structure and Bending Strength of Concrete under a High-low Temperature Cycle Based on Grey System Theory, *The Journal of Grey System*, *32(4)*, 7907 words.

Van Vlack, L.H. (1973), "Materials Science for Engineers", Addison Wesley, 4, USA.

Weyer, R.E., Prowell, B.D., Sprinkel, M.M., & Vorster, M. (1993), "Concrete Bridge Protection, Repair, and Rehabilitation Relative to Reinforcement Corrosion: A Methods Application". *Strategic Highway Research Program, National Research Council, Washington, National Academy of Sciences*, 1-263.

Wikipedia, Available from: https://www.builderspace.com/can-concrete-dry-underwater

Wyrzykowski, M., Gajewicz-Jaromin, A.M., Mc Donald, P.J., Dunstan, D.J., Scrivener, K.L., & Lura, P. (2019), Water Redistribution-Microdiffusion in Cement Paste under Mechanical Loading Evidenced by H NMR, *Journal of Physical Chemistry*, **123** (26), 16153-16163.